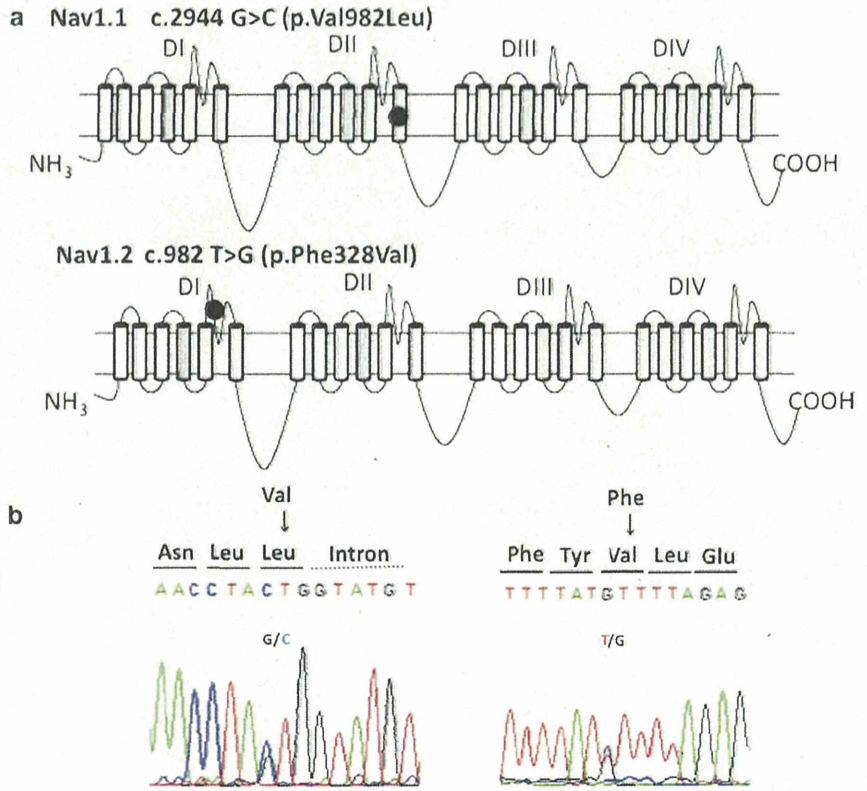

Fig. 2. Cases with *SCN1A* and *SCN2A* mutations in AET. (a) Structure of SCN1A ($Na_V1.1$) and SCN2A ($Na_V1.2$) with localization of the mutation (closed circle). c.2944 G>C (p.Val982Leu) is localized in the transmembrane segment 6 of domain II in $Na_V1.1$, whereas c.982 T>G (p.Phe328Val) is localized in the loop between S5 and S6 of segment I in $Na_V1.2$. (b) Electropherogram of the mutations. Substitution of G with C at nucleotide position c.2944 of *SCN1A* resulted in a change from valine to leucine (left), whereas substitution of T with G at nucleotide position c.982 caused a change from phenylalanine to valine, Accession numbers of *SCN2A* and *SCN2A* are AF117907.1 and Q99250, respectively.

epilepticus was refractory to anticonvulsants and lasted more than 15 min, requiring general anesthesia and mechanical ventilation for 6 days. Two days after extubation, he had a cluster of seizures presenting with apnea, staring, and bradycardia. At the age of 3, he started to take carbamazepine for complex partial seizures. Although cranial CT was normal in the acute phase, bilateral hippocampal sclerosis was revealed at follow-up cranial MRI imaging at 4 years and 1 month. He was eventually left with pervasive developmental disorders, mental deficiency and complex partial seizures. Neither myoclonic seizures nor generalized spike-wave discharges were noted during the follow-up period. Despite the presence of compatible clinical signs (biphasic seizures), the atypical CT/MRI findings rendered the diagnosis of AESD equivocal ("possible" AESD) in this case.

4. Discussion

This study elucidated the relationship between AET and AESD from both clinical and genetic viewpoints. The clinical picture of AESD has recently been well delineated [8,10]. The initial manifestation of AESD is a prolonged convulsive seizure triggered by acute febrile infection. In typical cases, the seizure is followed by post-ictal coma on day 1, and by recovery of consciousness on day 2. Cranial CT/MRI findings are normal at this stage. On day 3–9, however, there is a cluster of brief partial seizures, followed by a second coma. CT/MRI studies at this stage disclose cerebral cortical edema. Although the topography of cerebral lesions varies among patients, many of them show lobar (e.g. bilateral frontal) or hemispheric distribution. The peri-Rolandic regions (pre- and post-central gyri) are spared in many cases. The lesions are hypodense on CT and hyperintense on T2-weighted images of MRI. The most sensitive sequence is diffusion-weighted imaging, which visualizes restricted diffusion of the subcortical white matter, a characteristic pattern called a bright tree appearance. This finding provides strong evidence for the diagnosis of AESD. After the second coma, there are signs of cerebral cortical dysfunction, such as intellectual deficits, motor paralysis and epileptic seizures.

Please cite this article in press as: Saitoh M et al. Clinical and genetic features of acute encephalopathy in children taking theophylline. Brain Dev (2014), http://dx.doi.org/10.1016/j.braindev.2014.07.010

In convalescence, CT/MRI shows atrophy of the affected cortical regions. As many as 66% of patients are eventually left with neurological sequelae, in contrast to the low fatality of 1% [16].

In typical cases of AESD, the diagnosis is made easily, based on the characteristic clinical course (biphasic seizures) and MRI findings (bright tree appearance). In very severe cases, however, the diagnosis is often difficult for the following reasons. At onset, these cases usually have very persistent (more than 1 h) and intractable status epilepticus, and undergo intensive treatment, including continuous infusion of a large dose of intravenous barbiturate and brain hypothermia. There is neither recovery of consciousness on day 2 nor recurrence of partial seizures on day 3–9. Thus, the biphasic clinical course is not recognized. In addition, the critical condition of patients, as well as multiple lines for monitoring and tubes for ventilation and infusion, often renders MRI studies difficult and unsafe. Even in such cases, diagnosis of AESD may be made on the basis of CT findings, such as delayed cerebral edema, lobar or hemispheric involvement and peri-Rolandic sparing. Occasionally, the latter two features are first recognized by follow-up MRI during convalescence.

In this study on AET, we often encountered the same diagnostic problems. Nevertheless, we could make a diagnosis of AESD in 12 out of 16 cases (definite in 9 and probable in 3), by identifying either or both of the neurological and imaging features (Table 1, Fig. 1). The diagnosis of AESD was equivocal in 3 cases (possible AESD), and unlikely in one case (Case 12) that showed early cerebral edema (on day 1), multiorgan failure and fatal outcome. All these findings are very rare in AESD.

In this study, we revealed for the first time the genetic background of AET, focusing on the genes associated with AESD: *CPT2*, *ADORA2A*, *SCN1A* and *SCN2A*. Fifteen out of 16 patients had at least one of the following genotypes: polymorphism of *CPT2* (352C) and *ADORA2A* (hapolotype A), and mutation of *SCN1A* and *SCN2A*.

CPT2 is a mitochondrial enzyme essential for the metabolism of fatty acids and the resultant production of ATP. Certain polymorphisms of the *CPT2* gene cause thermolability, a sharp decline in enzymatic activity at high body temperature (e.g. 41 °C). Previous studies in Japan have demonstrated that CPT2 thermolabile variations predispose children to influenza-associated encephalopathy [20]. In particular, F352C, a typical variation, is a risk factor for AESD [12]. Interestingly, the [1055T>G/F352C] substitution has been reported only in East Asians and not in Caucasians (rs2229291 on NCBI, http://www.sanger.ac.uk/), which partially accounts for the high incidence of AESD in Japanese. In this study, we found that half of the AET cases (8 out of 16) had F352C, suggesting the role of CPT2 thermolability in the pathogenesis of AET.

ADORA2A is a receptor coupled to a stimulatory G protein. On adenosine binding, ADORA2A stimulates adenylate cyclase to produce cyclic adenosine monophosphate (cAMP), which in turn facilitates calcium ion influx, glutamate release and neuronal excitation. Genetic variation of the *ADORA2A* gene is associated not only with caffeine sensitivity [21], but also with AESD. Haplotype A, a predisposing factor of AESD, causes high expression of the *ADORA2A* mRNA and ADORA2A protein, as well as high production of cAMP in response to adenosine, in an additive manner (diplotype AA>AB>BB) [13]. Thus, in the presence of haplotype A, the balance between inhibitory ADORA1 and stimulatory ADORA2A may shift to favor the latter. When combined with the non-selective inhibitory effects of theophylline for both the receptors [22], this altered balance may lead to the onset of acute encephalopathy. Indeed, this study found that the vast majority of cases (14 out of 16) had at least one haplotype A. Interestingly, two patients with diplotype AA had no other risk genotypes (regarding *CPT2*, *SCN1A* and *SCN2A*), whereas 10 out of the 12 patients with diplotype AB had another risk genotype. This study failed to show a statistically significant difference in the genotype distribution of *CPT2* and *ADORA2A* between AET and controls because of the small number of cases. A study involving a larger number of AET patients is necessary to further elucidate the genetic background.

SCN1A and SCN2A are voltage-gated sodium ion channels on the cell membrane of CNS neurons. Mutations of the *SCN1A* and *SCN2A* genes cause familial epileptic syndromes, such as Dravet syndrome and generalized epilepsy with febrile seizures plus (GEFS plus). Recently, the clinical spectrum of these mutations has widened considerably. We and other investigators have reported cases presenting clinically with syndromes of acute encephalopathy, such as AESD and AERRPS, but not with Dravet's syndrome or GEFS plus [14,15]. In this study of AET, we found two patients: Case 2 with V982L of *SCN1A*, and Case 14 with F328V of *SCN2A*. The former patient had typical AESD, whereas the latter showed bilateral hippocampal sclerosis, an MRI finding atypical for AESD. In this context, a recent animal experiment has shown that aminophylline at the usual doses aggravates hypoxia-induced injury of hippocampal neurons [23]. It is plausible that mutations of the *SCN1A* and *SCN2A* genes, when combined with the multiple effects of theophylline, lead to variable neurological phenotypes, including AESD and other encephalopathies.

In summary, our clinical and genetic studies of Japanese patients with AET revealed that AET overlaps with AESD. Of the 16 AET cases, 12 met the diagnostic criteria of AESD, and 14 had at least one gene polymorphism or mutation previously known as genetic risk factors of AESD.

Please cite this article in press as: Saitoh M et al. Clinical and genetic features of acute encephalopathy in children taking theophylline. Brain Dev (2014), http://dx.doi.org/10.1016/j.braindev.2014.07.010

Acknowledgement

Dr. Saitoh is funded by a Grant-in-Aid for Scientific Research from the Japan Society for the Promotion of Science No. 24390258 and by a Grant-in-Aid for research on Measures for Intractable Diseases H25-Nanjitou-Ippan-009 from the Ministry of Health, Labour and Welfare, Japan. Dr. Ishii is funded by a Grant-in-Aid for Young Scientists (B) (23791201), Grants for Scientific Research on Innovative Areas (221S0002 and 25129708). Dr. Hirose is funded by a Grant-in-Aid for Grant-in-Aid for Scientific Research (A) (24249060), Grant-in-Aid for Challenging Exploratory Research (25670481), Bilateral Joint Research Projects from Japan Society for the Promotion of Science (JSPS), Grants for Scientific Research on Innovative Areas (221S0002 and 25129708) from the Ministry of Education, Culture, Sports, Science, and Technology (MEXT), MEXT-supported Program for the Strategic Research Foundation at Private Universities 2013-2017, a Grant-in-aid for the Research on Measures for Intractable Diseases (No. H23-Nanji-Ippan-78) from the Ministry of Health, Labor and Welfare, Intramural Research Grant (24-7) for Neurological and Psychiatric Disorders of NCNP, the Joint Usage/Research Program of Medical Research Institute, Tokyo Medical and Dental University, Grants from The Mitsubishi Foundation and Takeda Scientific Foundation, 2013–2017 "Research grants for Central Research Institute for the Molecular Pathomechanisms of Epilepsy of Fukuoka University", Recommended Projects of Fukuoka University (117016) Nervous and Mental Disorder Grand 24-7 and H24-Nanji-Ippan-29 from the Ministry of Health, Labour and Welfare, Japan. Dr. Mizuguchi is funded by a Grant-in-Aid for Scientific Research from the Japan Society for the Promotion of Science No. 24390258 and by a Grant-in-Aid for research on Measures for Intractable Diseases H25-Nanjitou-Ippan-009 from the Ministry of Health, Labour and Welfare, Japan.

References

[1] Tsiu SJ, Self TH, Burns R. Theophylline toxicity: update. Ann Allergy 1990;64:241–57.
[2] Miura T, Kimura K. Theophylline-induced convulsions in children with epilepsy. Pediatrics 2000;105:920.
[3] Dunwiddie TV. Endogenously released adenosine regulates excitability in the in vitro hippocampus. Epilepsia 1980;21:541–8.
[4] Dunwiddie TV. Adenosine and suppression of seizures. Adv Neurol 1999;79:1001–10.
[5] Korematsu S, Miyahara H, Nagakura T, Suenobu S, Izumi T. Theophylline-associated seizures and their clinical characterizations. Pediatr Int 2008;50:95–8.
[6] Nakada T, Kwee IL, Lerner AM, Remler MP. Theophylline-induced seizures: clinical and pathophysiologic aspects. West J Med 1983;138:371–4.
[7] Yoshikawa H. First-line therapy for theophylline-associated seizures. Acta Neurol Scand (Suppl) 2007;186:57–61.
[8] Mizuguchi M, Yamanouchi H, Ichiyama T, Shiomi M. Acute encephalopathy associated with influenza and other viral infections. Acta Neurol Scand (Suppl) 2007;186:45–56.
[9] Nabbout R, Vezzani A, Dulac O, Chiron C. Acute encephalopathy with inflammation-mediated status epilepticus. Lancet Neurol. 2011;10:99–108.
[10] Takanashi J, Oba H, Barkovich AJ, Tada H, Tanabe Y, Yamanouchi H, et al. Diffusion MRI abnormalities after prolonged febrile seizures with encephalopathy. Neurology 2006;66:1304–9.
[11] Shiomi M. A proposal of the clinical classification of influenza encephalopathy. (in Japanese). Jpn J Pediatr 2000;53:1739–46.
[12] Shinohara M, Saitoh M, Takanashi J, Yamanouchi H, Kubota M, Goto T, et al. Carnitine palmitoyl transferase II polymorphism is associated with multiple syndromes of acute encephalopathy with various infectious diseases. Brain Dev 2011;33:512–7.
[13] Shinohara M, Saitoh M, Nishizawa D, Ikeda K, Hirose S, Takanashi J, et al. ADORA2A polymorphism predisposes children to encephalopathy with febrile status epilepticus. Neurology 2013;80:1571–6.
[14] Saitoh M, Shinohara M, Hoshino H, Kubota M, Amemiya K, Takanashi J, et al. Mutations of the SCN1A gene in acute encephalopathy. Epilepsia 2012;53:558–64.
[15] Kobayashi K, Ohzono H, Shinohara M, Saitoh M, Ohmori I, Ohtsuka Y, et al. Acute encephalopathy with a novel point mutation in the SCN2A gene. Epilepsy Res 2012;102:109–12.
[16] Hoshino A, Saitoh M, Oka A, Okumura A, Kubota M, Saito Y, et al. Epidemiology of acute encephalopathy in Japan, with emphasis on the association of viruses and syndromes. Brain Dev 2012;34:337–43.
[17] Mizuguchi M. Influenza encephalopathy and related neuropsychiatric syndromes. Influenza Other Respir Viruses 2013;7:67–71.
[18] Singh NA, Pappas C, Dahle EJ, Claes LR, Pruess TH, De Jonghe P, et al. A role of SCN9A in human epilepsies, as a cause of febrile seizures and as a potential modifier of Dravet syndrome. PLoS Genet 2009;5:e1000649.
[19] Shi X, Yasumoto S, Nakagawa E, Fukasawa T, Uchiya S, Hirose S. Missense mutation of the sodium channel gene SCN2A causes Dravet syndrome. Brain Dev 2009;31:758–62.
[20] Chen Y, Mizuguchi H, Yao D, Ide M, Kuroda Y, Shigematsu Y, et al. Thermolabile phenotype of carnitine palmitoyltransferase II variations as a predisposing factor for influenza-associated encephalopathy. FEBS Lett 2005;579:2040–4.
[21] Rogers PJ, Hohoff C, Heartherley SV, Mullings EL, Maxfield PJ, Evershed RP, et al. Association of the anxiogenic and alerting effects of caffeine with ADORA2A and ADORA1 polymorphisms and habitual level of caffeine consumption. Neuropsychopharmacology 2010;35:1973–83.
[22] Fukuda M, Suzuki Y, Hino H, Kuzume K, Morimoto T, Ishii E. Adenosine A1 receptor blockage mediates theophylline-associated seizures. Epilepsia 2010;51:483–7.
[23] Somekawa-Kondo T, Yamaguchi K, Ishitsuka Y, Ito S, Tanaka K, Irikura M, et al. Aminophylline, administered at usual doses for rodents in pharmacological studies, induces hippocampal neuronal cell injury under low tidal volume hypoxic conditions in guinea-pigs. J Pharm Pharmacol 2013;65:102–14.

Please cite this article in press as: Saitoh M et al. Clinical and genetic features of acute encephalopathy in children taking theophylline. Brain Dev (2014), http://dx.doi.org/10.1016/j.braindev.2014.07.010

Respiratory Physiology & Neurobiology 202 (2014) 16–23

Contents lists available at ScienceDirect

Respiratory Physiology & Neurobiology

journal homepage: www.elsevier.com/locate/resphysiol

Magnitude of influenza virus replication and cell damage is associated with interleukin-6 production in primary cultures of human tracheal epithelium

Mutsuo Yamaya [a,*], Lusamba K. Nadine [a], Chiharu Ota [a], Hiroshi Kubo [a], Tomonori Makiguchi [b], Ryoichi Nagatomi [c], Hidekazu Nishimura [d]

[a] Department of Advanced Preventive Medicine for Infectious Disease, Tohoku University Graduate School of Medicine, Sendai 980-8575, Japan
[b] Department of Respiratory Medicine, Tohoku University Graduate School of Medicine, Sendai 980-8575, Japan
[c] Medicine and Science in Sports and Exercise, Tohoku University Graduate School of Medicine, Sendai 980-8575, Japan
[d] Virus Research Center, Clinical Research Division, Sendai National Hospital, Sendai 983-8520, Japan

ARTICLE INFO

Article history:
Accepted 15 July 2014
Available online 23 July 2014

Keywords:
Airway epithelial cells
Cell damage
Influenza virus
Interleukin-6
Pathogenicity

ABSTRACT

Primary cultures of human tracheal epithelium were infected with influenza viruses to examine the relationships between the magnitude of viral replication and infection-induced cell damage and cytokine production in airway epithelial cells. Infection with four strains of the type A influenza virus increased the detached cell number and lactate dehydrogenase (LDH) levels in the supernatants. The detached cell number and LDH levels were related to the viral titers and interleukin (IL)-6 levels and the nuclear factor kappa B (NF-κB) p65 activation. Treatment of the cells with an anti-IL-6 receptor antibody and an NF-κB inhibitor, caffeic acid phenethyl ester, reduced the detached cell number, viral titers and the LDH levels and improved cell viability after infection with the pandemic influenza virus [A/Sendai-H/N0633/2009 (H1N1) pdm09]. A caspase-3 inhibitor, benzyloxycarbonyl-DEVD-fluoromethyl ketone, reduced the detached cell number and viral titers. Influenza viral infection-induced cell damage may be partly related to the magnitude of viral replication, NF-κB-p65-mediated IL-6 production and caspase-3 activation.

1. Introduction

The high virulence of the influenza virus causes severe illness and increases the fatality rate in patients. Precise information regarding the pathogenic magnitude of the influenza viruses is needed for the effective treatment of influenza viral infection and for the prevention of confusion and fear during a pandemic infection. The pathogenic magnitude of the influenza virus has been reported to be associated with the non-structural (NS) gene segment of the influenza A (H5N1) virus (Cheung et al., 2002), contributing to the increase in inflammatory cytokine production. Furthermore, several studies have reported mechanisms of the high pathogenicity, which include the elevation in pulmonary concentrations of inflammatory cytokines, including interleukin (IL)-1, IL-6 and interferon (IFN)-γ, the decrease in anti-inflammatory cytokine production and the elevation in viral replication (de Jong et al., 2006; Lipatov et al., 2005). Influenza viral infection induces viral replication, cytokine production and cell damage in the airway epithelium, which is the first target of the infection. However, the mechanisms and relationship between viral replication, cytokine production and cell damage in the human airway epithelium have not been well studied.

Influenza viral infection-induced production of inflammatory cytokines, including IL-6 and tumor necrosis factor (TNF)-α, and proteases may cause damage to airway and alveolar epithelial cells and vascular endothelial cells (Mauad et al., 2010; Ruwanpura et al., 2011; Wang et al., 2010) and may subsequently exacerbate bronchial asthma and chronic obstructive pulmonary disease, and develop acute respiratory distress syndrome (Nicholson et al., 1993; Perez-Padilla et al., 2009; Rohde et al., 2003). IL-6 and TNF-α are associated with cell death and the activation of caspases in swine macrophages after pandemic A/H1N1 viral infection (Gao et al., 2012). However, the mechanisms for cytokine production-induced airway cell damage resulting from influenza viral infection have not been well studied.

* Corresponding author. Tel.: +81 22 717 7184; fax: +81 22 717 7576.
E-mail address: myamaya@med.tohoku.ac.jp (M. Yamaya).

http://dx.doi.org/10.1016/j.resp.2014.07.010
1569-9048/

Primary cultures of human tracheal epithelial cells may demonstrate the real pathogenic influence of influenza viral infection on the damage, viral replication and inflammatory cytokine production in the airways because human tracheal epithelial cells cultured using the method that we reported previously (Yamaya et al., 1992) retain the functions of the original tissue. In the present study, we infected primary cultures of human tracheal epithelial cells with four strains of influenza virus and measured the magnitude of viral replication, cell damage and cytokine production. We also examined the relationships and mechanisms among viral replication, cell damage and cytokine production in the infection with the pandemic influenza virus [A/Sendai-H/N0633/2009 (H1N1) pdm09].

2. Materials and methods

2.1. Human tracheal epithelial cell culture

The isolation and culture of the human tracheal surface epithelial cells were performed as described previously (Yamaya et al., 2010) in a mixture of Dulbecco's modified Eagle's medium (DMEM)-Ham's F-12 (DF-12) medium containing 2% Ultroser G (USG) serum substitute. The tracheas used for the cell cultures were obtained from 23 patients after death (age, 72 ± 11 yr; 10 female and 13 male). This study was approved by the Tohoku University Ethics Committee.

2.2. Culture of Madin Darby Canine Kidney cells

Madin Darby Canine Kidney (MDCK) cells were cultured in T_{25} flasks in Eagle's minimum essential medium (MEM) containing 10% fetal calf serum (Numazaki et al., 1987; Yamaya et al., 2010). The cells were then plated in 96-well plates and cultured.

2.3. Viral stocks

Stocks of influenza viruses were generated by infecting human tracheal epithelial cells with four strains of influenza virus as follows: the pandemic A/H1 2009 virus [A/H1N1 pdm 2009, A/Sendai-H/N0633/2009 (H1N1) pdm09] and three strains of the human influenza virus [A/H1N1 Sendai, A/Sendai-H/108/2009/(H1N1); A/H3N2 New York, A/H3N2/New York/55/2004; A/H3N2 Aichi, A/Aichi/2/68 (H3N2)] (Yamaya et al., 2010). The cells were cultured in 24-well plates in 0.9 ml of DF-12 medium and 100 μl of MEM containing virus for 1 h. The culture supernatants containing virus were then removed, and the cells were cultured in DF-12 medium containing 2% USG at 37 °C in 5% CO_2-95% air. To obtain the influenza virus solution, the supernatants were collected.

To prepare the A/H1N1 pdm 2009 virus and the A/H1N1 Sendai virus, which was isolated during the 2008–2009 season, nasal swabs were collected from patients and suspended in MEM medium (Numazaki et al., 1987). The A/H3N2 New York virus and the A/H3N2 Aichi virus, which were passaged 5–7 times in MDCK cells, were also used for the generation of viral stocks.

2.4. Detection and titration of viruses

The detection and titration of influenza viruses in the culture supernatant were performed using the endpoint method (Condit, 2006) by infecting replicate MDCK cells in plastic 96-well plates with 10-fold dilutions of virus-containing supernatants, as previously described (Yamaya et al., 2010). The presence of the typical cytopathic effects of the influenza virus was then examined. The $TCID_{50}$ (TCID, tissue culture infective dose) was calculated using previously described methods (Condit, 2006), and the viral titers in the supernatants were expressed as $TCID_{50}$ units/ml (Yamaya et al., 2010).

2.5. Viral infection of the cells

The infection of human tracheal epithelial cells with influenza was performed using previously described methods (Yamaya et al., 2010). A stock solution of influenza virus was added to the cells in 24-well plates (400 μl in each well, 1.0×10^3 $TCID_{50}$ units/ml, 0.8×10^{-3} $TCID_{50}$ units/cell of the multiplicity of infection). After a 1-h incubation period, the viral solution was removed, and the cells were cultured in 1 ml of fresh medium at 37 °C in 5% CO_2-95% air.

2.6. Collection of the supernatants

The supernatant (300 μl) was collected 1 day (24 h) and 3 days (72 h) after infection, and the same volume (300 μl) of fresh medium was added. The entire supernatant volume (1 ml) was collected 5 days (120 h) after infection. Furthermore, when the influenza virus titers 7 days (168 h) after infection were measured, the supernatant (300 μl) was collected 1 day (24 h), 3 days (72 h) and 5 days (120 h) after infection, and the same volume (300 μl) of fresh medium was added. The entire supernatant volume (1 ml) was collected 7 days (168 h) after infection.

2.7. Measurement of airway epithelial cell damage

To examine the tracheal epithelial cell damage after influenza infection, the number of floating cells in the supernatants, which were detached from the cell sheets adhered on the culture vessels of 24-well plates, and the number and viability of the adhered cells were measured by trypan blue exclusion. Lactate dehydrogenase (LDH) concentrations in the supernatants were also measured. These parameters demonstrate apoptosis and necrosis (Catalani et al., 2013; Cechetti et al., 2007; Yan et al., 2013).

2.8. Quantification of influenza virus RNA

Viral RNA in the cells was measured to confirm differences in the magnitude of viral replication among the species. A two-step real-time quantitative reverse transcription (RT)-PCR was performed using the TaqMan® Gene Expression Master Mix (Applied Biosystems, Bedford, CA, USA) as described previously (Yamaya et al., 2010). The primers and TaqMan probe for the viruses were designed as previously reported (Lorusso et al., 2010; Yamaya et al., 2010). The expression of viral RNA was normalized to the constitutive expression of β-actin mRNA (Suzuki et al., 2002).

2.9. NF-kappa B assay

The presence of p50 and p65 subunits in the nuclear extracts was assayed using a TransFactor Family Colorimetric Kit-NF-κB (BD Bioscience/CLONTECH) as previously described (Yamaya et al., 2011).

2.10. Measurement of cytokine production

We measured IL-6, TNF-α and IFN-γ levels in the supernatants. The measurement of IL-6 and INF-γ was performed using specific enzyme-linked immunosorbent assays (ELISA), and the measurement of TNF-α was performed using chemiluminescent enzyme immunoassay.

2.11. Statistical analysis

The results are expressed as the mean ± SEM. The statistical analysis was performed using a two-way repeated measures

analysis of variance (ANOVA). Subsequent post-hoc analyses were performed using Bonferroni's method. For all of the analyses, values of $p < 0.05$ were assumed to be significant. In the experiments using human tracheal epithelial cell cultures, n refers to the number of donors (tracheae) from which the cultured epithelial cells were obtained.

3. Results

3.1. Influenza virus release from airway epithelial cells

All four influenza virus strains that were tested, including the pandemic A/H1N1 2009 virus (A/H1N1 pdm 2009) and three strains of type A seasonal human influenza virus (A/H1N1 Sendai, A/H3N2 New York and A/H3N2 Aichi), were detected in the supernatants at 24 h, and the viral titers increased progressively between 24 h and 3 days after infection (Fig. 1A). The influenza virus titers of the four strains in the supernatants increased with time during the 3 days of observation ($p < 0.05$ in each case by ANOVA), and consistent viral titers were observed for 5 days after infection (Fig. 1A). Furthermore, consistent titers of the four strains of type A influenza virus were observed between day 5 and day 7. By contrast, the influenza viral titers of the four strains in the supernatants started to decline on day 7 after infection ($p < 0.05$). The influenza viral titers of the four strains 7 days after infection were as follows (mean ± SEM, $n = 5$): 5.6 ± 0.4 for the A/H1N1 pdm 2009 virus, 5.2 ± 0.4 for the A/H1N1 Sendai virus, 3.1 ± 0.3 for the A/H3N2 New York virus and 1.2 ± 0.3 for the A/H3N2 Aichi virus.

The viral titers of the A/H1N1 pdm 2009 virus and the A/H1N1 Sendai virus were higher than the titers of the A/H3N2 New York virus and the A/H3N2 Aichi virus (Fig. 1A and B). Furthermore, the titers of the A/H3N2 New York virus were higher than those of the A/H3N2 Aichi virus (Fig. 1A and B).

3.2. The number of detached cells after influenza viral infection

The number of detached cells in the supernatants 5 days after the sham infection with the DF-12 medium containing 2% USG was $0.8 \pm 0.1 \times 10^4$ (/well of 24-well plates, $n = 4$). The number of detached cells 5 days after the infection with four strains of virus was higher than the number of detached cells after the sham infection (Fig. 1C).

The number of detached cells after infection with the A/H1N1 pdm 2009 virus and the A/H1N1 Sendai virus was higher than the number after infection with the A/H3N2 New York virus and the A/H3N2 Aichi virus (Fig. 1C). Furthermore, the number of detached cells after infection with the A/H3N2 New York virus was higher than the number after infection with the A/H3N2 Aichi virus (Fig. 1C).

3.3. LDH release after influenza viral infection

The concentration of LDH in the supernatants 5 days after the sham infection was 34 ± 3 units/l ($n = 4$). The concentration of LDH 5 days after the infection with four strains of virus was higher than the concentration of LDH after the sham infection (Fig. 1D).

The concentration of LDH after the infection with the A/H1N1 pdm 2009 virus and the A/H1N1 Sendai virus were higher than the concentration of LDH after infection with the A/H3N2 New York virus and the A/H3N2 Aichi virus (Fig. 1D). The LDH levels after infection with the A/H3N2 New York virus were higher than the LDH levels after infection with the A/H3N2 Aichi virus (Fig. 1D).

3.4. Cytokine production after influenza viral infection

A significant amount of IL-6 in the supernatants was detected before viral infection (211 ± 13 pg/ml, $n = 4$) and 5 days after sham infection (Fig. 1E). The IL-6 levels increased after infection with the four strains of influenza virus (Fig. 1E). Maximum IL-6 levels were observed 5 days after infection with the four strains of influenza virus (data at 1 day, 3 days and 7 days not shown).

The IL-6 levels after infection with the A/H1N1 pdm 2009 virus and the A/H1N1 Sendai virus were higher than the IL-6 levels after infection with the A/H3N2 New York virus and the A/H3N2 Aichi virus (Fig. 1E). Furthermore, the IL-6 levels after infection with the A/H3N2 New York virus were higher than the levels after infection with the A/H3N2 Aichi virus (Fig. 1E).

In contrast, the concentration of TNF-α in the supernatants before infection was below the limits of detection (<0.55 pg/ml). TNF-α levels increased after infection with the four strains of virus, and significant amounts of TNF-α were detected after viral infection. TNF-α levels increased after infection with the four strains of virus as follows: 20 ± 2 pg/ml ($n = 4$) in the A/H1N1 pdm 2009 virus, 23 ± 2 pg/ml ($n = 4$) in the A/H1N1 Sendai virus, 11 ± 2 pg/ml ($n = 4$) in the A/H3N2 New York virus and 3 ± 1 pg/ml ($n = 4$) in the A/H3N2 Aichi virus. TNF-α levels after infection with the A/H1N1 pdm 2009 virus and the A/H1N1 Sendai virus were higher than the levels after infection with the A/H3N2 New York virus and the A/H3N2 Aichi virus ($p < 0.05$). The TNF-α levels after infection with the A/H3N2 New York virus were higher than the levels after infection with the A/H3N2 Aichi virus ($p < 0.05$).

The concentration of IFN-ϒ, measured using ELISA method, was below the limits of detection (<0.69 pg/ml).

3.5. NF-κB activation after influenza viral infection

A significant amount of the NF-κB p50 and p65 subunits was detected in the nuclear extracts from the vehicle-treated cells without influenza viral infection (Fig. 2). Infection with four strains of the influenza virus increased the amounts of the p50 and p65 subunits 5 days after infection (Fig. 2).

Significant differences in the amounts of NF-κB p50 in nuclear extracts were not observed among the cells infected with the four strains of influenza virus (Fig. 2A).

In contrast, the amounts of NF-κB p65 after infection with the A/H1N1 pdm 2009 virus and the A/H1N1 Sendai virus were higher than the amounts in the cells infected with the A/H3N2 New York virus and the A/H3N2 Aichi virus (Fig. 2B). Furthermore, the amounts of NF-κB p65 after infection with the A/H3N2 New York virus were higher than the amounts after infection with the A/H3N2 Aichi virus (Fig. 2B).

3.6. Effects of NF-kappa B inhibitor, anti-IL-6 antibody and caspase-3 inhibitor

We also studied the roles of NF-κB, IL-6 and caspase-3 on A/H1N1 pdm 2009 viral infection-induced cell damage and viral replication. The cells were treated with either an NF-κB inhibitor, caffeic acid phenethyl ester (CAPE, Calbiochem, La Jolla, CA, USA; 1 μM) (Natajaran et al., 1996), a monoclonal anti-IL-6 receptor antibody (R & D Systems Inc, MN, USA, 1.0 μg/ml) (Hsu et al., 2011), or a caspse-3 inhibitor, benzyloxycarbonyl-DEVD-fluoromethyl ketone (Z-DEVD-fmk) (Bio Vision, 1 μM) (Nicholson et al., 1995) from 30 min prior to viral infection until the measurement of the functions after infection.

The A/H1N1 pdm 2009 viral infection increased the number of detached cells in the supernatants (Fig. 3A and B), increased the number of dead cells in the attached cells and reduced the viability of the attached cells (Fig. 3C and D), although the viability changes

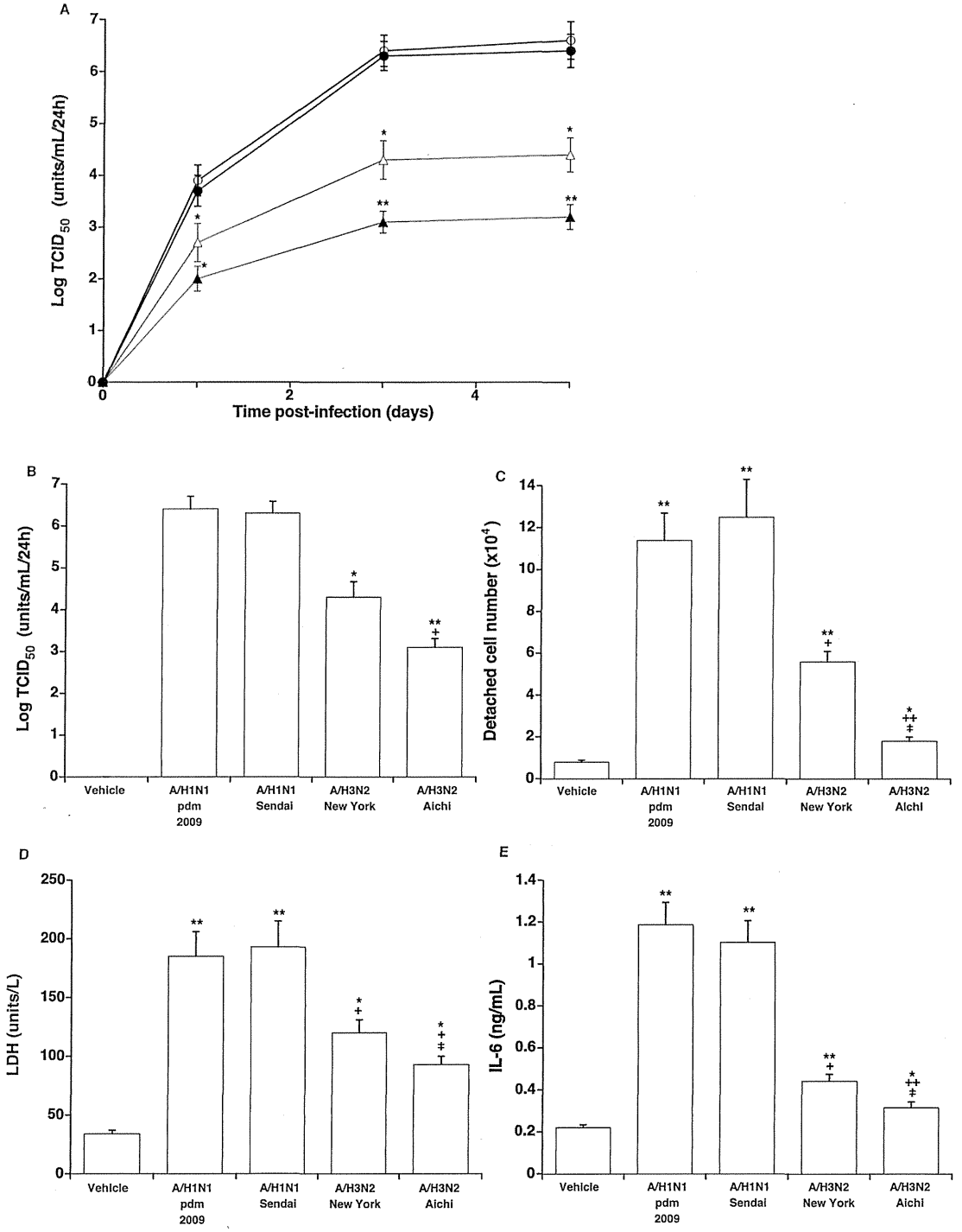

Fig. 1. (A) The time course of viral release into the supernatants of primary cultures of human tracheal epithelial cells obtained at different times after exposure to A/H1N1 pdm 2009 (open circles), A/H1N1 Sendai (closed circles), A/H3N2 New York (open triangles) and A/H3N2 Aichi (closed triangles) influenza viruses. Changes in the virus concentration in the supernatants are expressed as $TCID_{50}$ units/ml/24 h. The results are expressed as the mean ± SEM from four different tracheae. (B) Viral titers in the supernatants 5 days after exposure to the A/H1N1 pdm 2009, A/H1N1 Sendai, A/H3N2 New York and A/H3N2 Aichi viruses. Changes in the virus concentration in the supernatants are expressed as $TCID_{50}$ units/ml/24 h. The results are expresses as the mean ± SEM from four different tracheae. Significant differences from infection with the A/H1N1 pdm 2009 virus and the A/H1N1 Sendai virus are indicated by * $p < 0.05$ and ** $p < 0.01$. Significant differences from infection with the A/H3N2 New York virus are indicated by $^{+}$ $p < 0.05$. (C)–(E): The number of detached cells (C), concentration of LDH (D) and IL-6 (E) in the supernatants 5 days after exposure to the A/H1N1 pdm 2009, A/H1N1 Sendai, A/H3N2 New York and A/H3N2 Aichi viruses. The results are expressed as the mean ± SEM from four different tracheae. Significant differences from the sham infection (Vehicle) are indicated by * $p < 0.05$ and ** $p < 0.01$. Significant differences from infections with the A/H1N1 pdm 2009 virus and the A/H1N1 Sendai virus are indicated by $^{+}$ $p < 0.05$ and $^{++}$ $p < 0.01$. Significant differences from infection with the A/H3N2 New York virus are indicated by ‡ $p < 0.05$.

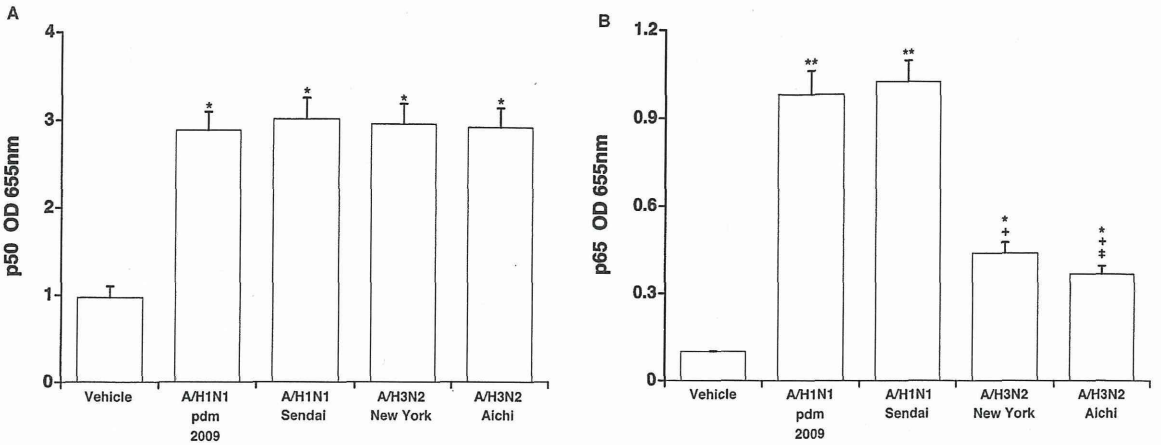

Fig. 2. (A) and (B) Amount of p50 (A) and p65 (B) in the nuclear extracts of cells 5 days after exposure to the A/H1N1 pdm 2009, A/H1N1 Sendai, A/H3N2 New York and A/H3N2 Aichi viruses. The results are expressed as the optical density (OD) and are the means ± SEM from four tracheae. Significant differences from the sham infection (Vehicle) are indicated by * $p < 0.05$ and ** $p < 0.01$. Significant differences from infections with the A/H1N1 pdm 2009 virus and the A/H1N1 Sendai virus are indicated by + $p < 0.05$. Significant differences from infection with the A/H3N2 New York virus are indicated by ‡ $p < 0.05$.

were small. The virus infection also increased the LDH concentration in the supernatants (Fig. 3E). Treatment with CAPE reduced the number of detached cells (Fig. 3A and B), reduced the number of dead cells, increased the viability of the cells and reduced the concentration of LDH (Fig. 3C–E) after the viral infection.

Treatment with CAPE also slightly, but significantly, reduced the A/H1N1 pdm 2009 viral titers in the supernatants and the viral RNA in the cells compared with the viral titers and viral RNA in the vehicle-treated cells (0.005% ethanol) (Fig. 3F and G).

Treatment with a monoclonal anti-IL-6 receptor antibody reduced the number of detached cells (Fig. 3A and B), reduced the number of dead cells, increased the viability of the cells and reduced the concentration of LDH (Fig. 3C–E) after the viral infection. Similarly, a monoclonal anti-IL-6 receptor antibody reduced the A/H1N1 pdm 2009 viral titers and viral RNA compared with the viral titers and viral RNA in the vehicle-treated cells (Fig. 3F and G).

Treatment with Z-DEVD-fmk (1 μM) reduced the number of detached cells and viral titers in the supernatants, but did not affect the concentration of LDH (Table 1) after the viral infection. In contrast, treatment with 10 μM Z-DEVD-fmk (Wen et al., 2010) induced cell damage in the absence of viral infection.

4. Discussion

We demonstrated that infection with four strains of type A influenza virus increased the detached cell number and the LDH levels in the supernatants of primary cultures of human tracheal epithelial cells. The detached cell number and the LDH levels were related to the viral titers, IL-6 levels and NF-κB p65 activation. Treatment with an NF-κB inhibitor (CAPE) (Natajaran et al., 1996) and an anti-IL-6 antibody reduced the detached cell number, dead cell number (in the attached cell sheets), LDH levels, viral titers and viral RNA, and improved the viability of the adhered cell sheets after the pandemic influenza virus infection. These findings suggest that influenza viral infection-induced cell damage may be partly associated with the magnitude of viral replication and subsequent NF-κB-p65-mediated IL-6 production.

Table 1
Effects of a caspase-3 inhibitor on the viral titers and the cell damage after influenza virus infection.

	A/H1N1 pdm 2009 + vehicle	A/H1N1 pdm 2009 + Z-DEVD-fmk
Viral titer ($TCID_{50}$ units/ml/24 h)	6.5 ± 0.3	5.6 ± 0.2*
Detached cell number (×10^4)	10.3 ± 0.8	5.5 ± 0.5*
LDH (units/l)	188 ± 10	194 ± 6

The results are expressed as the mean ± SEM from three different tracheae. Human tracheal epithelial cells were treated with a caspse-3 inhibitor Z-DEVD-fmk (1 μM) or vehicle (0.5% DMSO, dimethyl sulfoxide). Significant differences from the viral infection alone (A/H1N1 pdm 2009 + vehicle) are indicated by * $p < 0.05$.

IL-6 is associated with the pathogenesis of emphysematous changes through lung apoptosis in mice (Ruwanpura et al., 2011). IL-6 and TNF-α are also associated with cell death and the activation of caspases in swine macrophages after pandemic A/H1N1 viral infection (Gao et al., 2012). In contrast, in the present study, the IL-6 levels (>1 ng/ml) were much higher than the TNF-α levels (<0.03 ng/ml). A monoclonal anti-IL-6 receptor antibody and a NF-κB inhibitor (CAPE) partly reduced the detached cell number, dead cell number (of the adhered cell sheets) and LDH levels, and improved the viability of the adhered cell sheets. The concentration of IFN-γ was below the limits of detection. These findings suggest that IL-6 might be partly associated with cell damage after an influenza viral infection. However, the roles of other factors and mediators that are produced influenza viral infection, including IL-1β, IL-8 (Yamaya et al., 2010) and reactive oxygen species (Kim et al., 2013), remains to be examined; however, conflicting effects of IL-1β on apoptosis (Coulter et al., 2002; Lu et al., 2014) and the anti-apoptotic effects of IL-8 (Gyanchandani et al., 2013) have been demonstrated.

The NS1 protein coded in the non-structural (NS) gene-segment acts to inhibit the host interferon response, leads to the high expression of TNF-α and enhances the virulence of the H5N1 virus (Cheung et al., 2002; Garcia-Sastre et al., 1998). By contrast, the NS1 protein of the A/H1N1 2009 virus differs from the protein of H5N1 with high virulence (Shelton et al., 2012). These characteristics are consistent with a report stating that the virulence of the pandemic influenza virus was not extremely high compared with the virulence of seasonal influenza viruses (Presanis et al., 2009) and that the virulence may be associated with similar cytotoxic effects of the A/H1N1 pdm 2009 and A/H1N1 Sendai viruses, as observed in the present study.

The reasons why an anti-IL-6 receptor antibody and CAPE reduced viral release and viral RNA replication are uncertain. However, IL-6 activates caspases (Cai et al., 2012) that enhance the release of viral ribonucleoprotein complexes from the nucleus (Wurzer et al., 2003). A caspase-3 inhibitor Z-DEVD-fmk reduced the A/H1N1 pdm 2009 viral titers in the supernatants in the present study. Acetylsalicylic acid also blocks influenza viral propagation via its NF-κB-inhibiting activity (Mazur et al., 2007). The IL-6

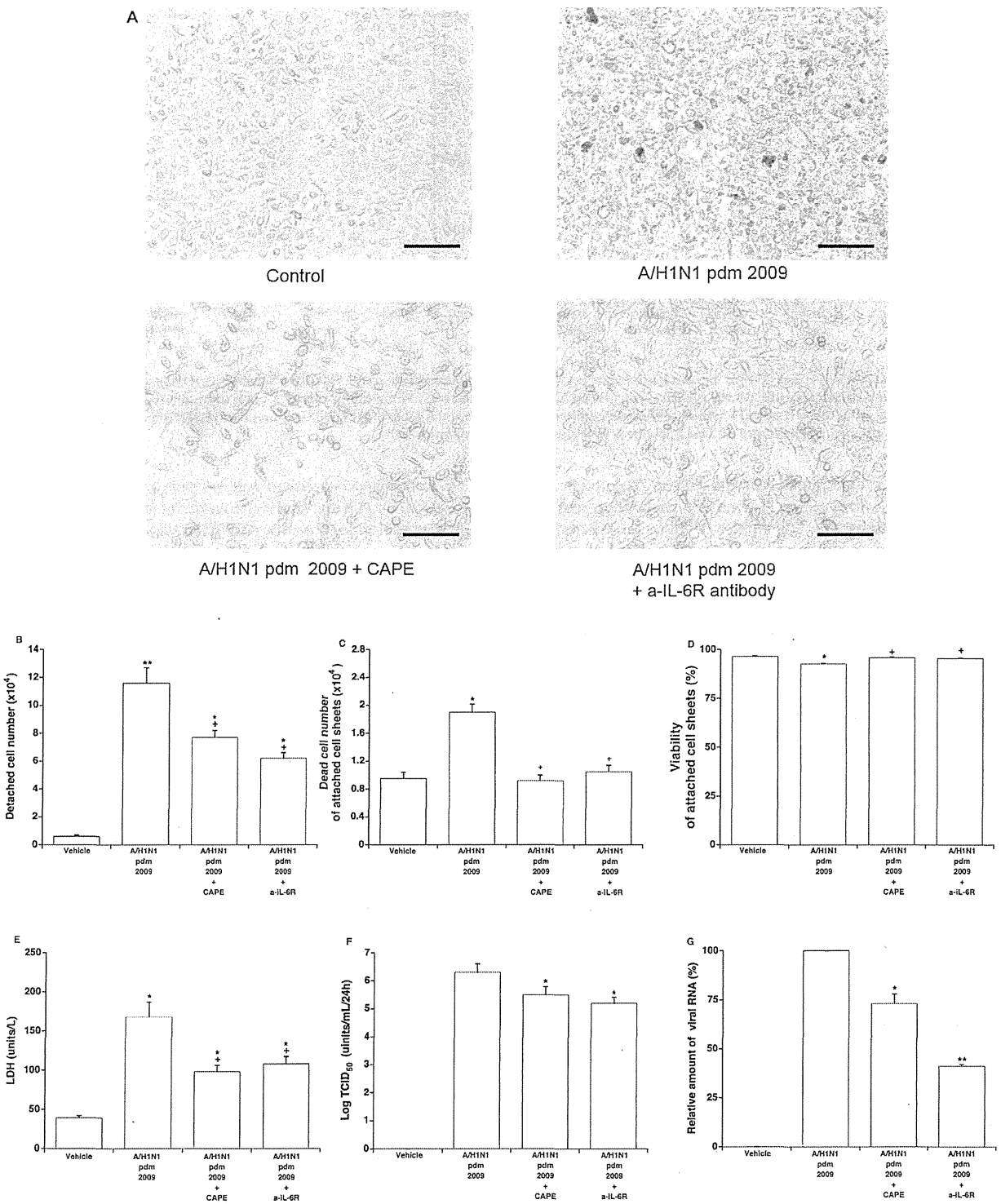

Fig. 3. (A) Phase contrast photographs of the primary cultures of human tracheal epithelial cells 5 days after infection with the A/H1N1 pdm 2009 virus and the vehicle (Control) in the presence of CAPE (A/H1N1 pdm 2009 + CAPE), a monoclonal anti-IL-6 receptor antibody (A/H1N1 pdm 2009 + a-IL-6R antibody) or vehicle (A/H1N1 pdm 2009). The surfaces of the confluent adhered cell sheets were covered with many detached floating cells from the sheets that were infected with the pandemic influenza virus (A/H1N1 pdm 2009). Treatment with CAPE and a monoclonal anti-IL-6 receptor antibody reduced the number of floating cells. Bar = 25 μm. (B)–(E): The number of detached cells (B), the number of dead cells and viability of adhered cell sheets ((C) and (D)), and the concentration of LDH (E) in the supernatants 5 days after exposure to the A/H1N1 pdm 2009 virus in the presence of CAPE (1 μM, A/H1N1 pdm 2009 + CAPE), an anti-IL-6 receptor antibody (1 μg/ml, A/H1N1 pdm 2009 + a-IL-6R) or the vehicle (A/H1N1 pdm 2009) or after the sham infection (Vehicle). The results are expressed as the mean ± SEM from four different tracheae. Significant differences from the sham infection are indicated by * $p < 0.05$ and ** $p < 0.01$. Significant differences from the viral infection alone are indicated by $^{+}$ $p < 0.05$. (F) and (G): Viral titers (F) in the supernatants and viral RNA (G) in the cells 5 days after exposure to the A/H1N1 pdm 2009 virus in the presence of CAPE (1 μM, A/H1N1 pdm 2009 + CAPE) or anti-IL-6 receptor antibody (1 μg/ml, A/H1N1 pdm 2009 + a-IL-6R) or exposure to the vehicle. Changes in the viral titers in the supernatants are expressed as $TCID_{50}$ units/ml/24 h. Viral RNA is expressed as the relative amount of RNA expression (%) compared with that of maximum viral RNA at day 5 in cells treated with the vehicle (A/H1N1 pdm 2009). The expression of viral RNA was normalized to the constitutive expression of β-actin mRNA. The results are expressed as the mean ± SEM from four different tracheae. Significant differences from the viral infection alone are indicated by * $p < 0.05$ and ** $p < 0.01$.

production may have enhanced influenza viral replication through NF-κB activation in the present study.

Infection with all of the four species of influenza virus activated both the NF-κB p50 and p65 subunits. Furthermore, the magnitude of p65 activation was associated with the magnitude of viral release, IL-6 production and the cell damage; however precise reasons are still uncertain regarding why only the p65 activation was associated with the magnitude of these factors. NF-κB increases the expression of genes for various pro-inflammatory cytokines (Zhu et al., 1996), and the production of interleukins is also associated with NF-κB p65 activation (Antal et al., 1996; More et al., 2013).

Influenza viral infection induces apoptosis through intrinsic and extrinsic pathways (Gao et al., 2013). The intrinsic pathway is mediated by members of the B-cell CLL/lymphoma 2 (Bcl-2) family and an apoptotic gene (Takizawa et al., 1993), and the extrinsic pathway is triggered by TNF family members (Gao et al., 2013). IL-6 is also associated with cell death and the activation of caspases in swine macrophages after pandemic A/H1N1 viral infection (Gao et al., 2012). In contrast, the induction of apoptosis of leukemia cells by suppressing NF-κB p65 has been reported (Ortiz-Lazareno et al., 2014). Partial inhibitory effects of the caspase-3 inhibitor on the cell detachment after virus infection, which were observed in the present study, may suggest the roles of caspase-3 activation induced by NF-κB-mediated-IL-6 production in the influenza viral infection-induced cell damage. However, we did not examine the effects of influenza virus infection on the activation of Bcl-2 family and apoptotic genes (Gao et al., 2013; Takizawa et al., 1993) in the present study. Further studies remain to clarify the mechanisms of cell damage after influenza virus infection.

The reason why the magnitude of virus replication was different among the four strains of virus is uncertain. However, virus stocks of the A/H1N1 pdm 2009 virus and the A/H1N1 Sendai virus were generated by infecting human tracheal epithelial cells with nasal swabs. In contrast, we generated virus stocks of the A/H3N2 New York virus and the A/H3N2 Aichi virus by infecting human tracheal epithelial cells with the viruses that had been passaged in MDCK cells. The serial passage of viruses in MDCK cells has been reported to reduce the potency of viral replication (Seladi-Schulman et al., 2013). The passage of viruses may influence the capability of virus replication.

In the present study, the titers of the four strains of type A influenza virus were detected for a prolonged duration of 7 days, which exceeds the duration reported by Boivin et al. (2000), who reported that significant viral titers in throat swabs were not detected 5 days (120 h) after the initiation of treatment with placebo. Although the reasons remain unclear, the absence of interferon in the supernatants, as demonstrated in the present study, might be partly associated with the long period of viral release from the cells in this study.

The dead cell number of attached cell sheets and the detached cell number and the LDH levels in the supernatants markedly increased after infection with A/H1N1 pdm 2009 virus in the present study. However, the viability measured by trypan blue exclusion was little affected. These results are consistent with those of Stark et al. (1991), who reported that LDH release is a more sensitive indicator of cell damage than trypan blue exclusion in human tracheal epithelial cells infected with parainfluenza viruses. These findings suggest that different assays may have different sensitivities for the detection of cell viability and cell damage after viral infection.

5. Conclusions

The magnitude of the detached cell number and the LDH levels in the supernatants of human tracheal epithelial cells was related to the magnitude of the replication of influenza viruses, the IL-6 production and the NF-κB p65 activation. Influenza viral infection-induced airway cell damage may be related to viral replication and subsequent NF-κB-p65-mediated IL-6 production.

Acknowledgements

This study was supported by Grant-in-Aid for Exploratory Research from Japan Society for the Promotion of Science (JSPS) KAKENHI Grant number 24659398.

References

Antal, J.M., Divis, L.T., Erzurum, S.C., Wiedemann, H.P., Thomassen, M.J., 1996. Surfactant suppresses NF-kappa B activation in human monocytic cells. Am. J. Respir. Cell Mol. Biol. 14, 374–379.

Boivin, G., Goyette, N., Hardy, I., Aoki, F., Wagner, A., Trottier, S., 2000. Rapid antiviral effect of inhaled zanamivir in the treatment of naturally occurring influenza in otherwise healthy adults. J. Infect. Dis. 181, 1471–1474.

Cai, Q., Lu, Z., Hong, G., Jiang, X., Wu, Z., Zheng, J., Song, Q., Chang, Z., 2012. Recombinant adenovirus Ad-RUNrf2 reduces paraquat-induced A549 injury. Hum. Exp. Toxicol. 31, 1102–1112.

Catalani, S., Carbonaro, V., Palma, F., Arshakyan, M., Galati, R., Nuvoli, B., Battistelli, S., Canestrari, F., Benedetti, S., 2013. Metabolism modifications and apoptosis induction after CellfoodTM administration to leukemia cell lines. J. Exp. Clin. Cancer Res. 32, 63.

Cechetti, F., Rhod, A., Simao, F., Santin, K., Salbego, C., Netto, C.A., Siqueira, I.R., 2007. Effect of treadmill exercise on cell damage in rat hippocampal slices submitted to oxygen and glucose deprivation. Brain Res. 1157, 121–125.

Cheung, C.Y., Poon, L.L.M., Lau, A.S., Luk, W., Lau, Y.L., Shortridge, K.F., Gordon, S., Guan, Y., Peiris, J.S.M., 2002. Induction of proinflammatory cytokines in human macrophages by influenza A (H5N1) viruses: a mechanism for the usual severity of human disease. Lancet 360, 1831–1837.

Condit, R.C., 2006. Principles of Virology. In: Knipe, D.M., Howley, P.M. (Eds.), Fields Virol, fifth ed. Lippincott Williams & Wilkins Inc., Philadelphia, PA, pp. 25–57.

Coulter, K.R., Doseff, A., Sweeney, P., Wang, Y., Marsh, C.B., Wewers, M.D., Knoell, D.L., 2002. Opposing effect by cytokines on Fas-mediated apoptosis in A549 lung epithelial cells. Am. J. Respir. Cell Mol. Biol. 26, 58–66.

de Jong, M.D., Simmons, C.P., Thanh, T.T., Hien, V.M., Smith, G.J., Chau, T.N., Hoang, D.M., Chau, N.V., Khanh, T.H., Dong, V.C., Qui, P.T., Cam, B.V., Ha, do Q., Guan, Y., Peiris, J.S., Chinh, N.T., Hien, T.T., Farrar, J., 2006. Fatal outcome of human influenza A (H5N1) is associated with high viral load and hypercytokinemia. Nat. Med. 12, 1203–1207.

Gao, R., Bhatnagar, J., Blau, D.M., Greer, P., Rollin, D.C., Denison, A.M., Deleon-Carnes, M., Shieh, W.J., Sambhara, S., Tumpey, T.M., Patel, M., Liu, L., Paddock, C., Drew, C., Shu, Y., Katz, J.M., Zaki, S.R., 2013. Cytokine and chemokine profiles in lung tissues from fatal cases of 2009 pandemic influenza A (H1N1): role of the host immune response in pathogenesis. Am. J. Pathol. 183, 1258–1268.

Gao, W., Sun, W., Qu, B., Cardona, C.J., Powell, K., Wegner, M., Shi, Y., Xing, Z., 2012. Distinct regulation of host responses by ERK and JNK MAP kinases in swine macrophages infected with pandemic (H1N1) 2009 influenza virus. PLoS One 7, e30328.

Garcia-Sastre, A., Egorov, A., Matassov, D., Brandt, S., Levy, D.E., Durbin, J.E., Palese, P., Muster, T., 1998. Influenza A virus lacking the NS1 gene replicates in interferon-deficient systems. Virology 252, 324–330.

Gyanchandani, R., Sano, D., Ortega Alves, M.V., Klein, J.D., Knapick, B.A., Oh, S., Myers, J.N., Kim, S., 2013. Interleukin-8 as a modulator of response to bevacizumab in preclinical models of head and neck squamous cell carcinoma. Oral Oncol. 49, 761–770.

Hsu, C.P., Chen, Y.L., Huang, C.C., Chou, C.C., Liu, C.L., Hung, C.H., Kao, T.Y., Chung, Y.C., 2011. Anti-interleukin-6 receptor antibody inhibits the progression in human colon carcinoma cells. Eur. J. Clin. Invest. 41, 277–284.

Kim, H.J., Kim, C.H., Ryu, J.H., Kim, M.J., Park, C.Y., Lee, J.M., Holtzman, M.J., Yoon, J.H., 2013. Reactive oxygen species induce antiviral innate immune response through IFN-regulation in human nasal epithelial cells. Am. J. Respir. Cell Mol. Biol. 49, 855–865.

Lipatov, A.S., Andreansky, S., Webby, R.J., Hulse, D.J., Rehg, J.E., Krauss, S., Perez, D.R., Doherty, P.C., Webster, R.G., Sangster, M.Y., 2005. Pathogenesis of Hong Kong H5N1 influenza virus NS gene reassortants in mice: the role of cytokines and B- and T-cell responses. J. Gen. Virol. 86, 1121–1130.

Lorusso, A., Faaberg, K.S., Killian, M.L., Koster, L., Vincent, A.L., 2010. One-step real-time RT-PCR for pandemic influenza A virus (H1N1) 2009 matrix gene detection in swine samples. J. Virol. Methods 164, 83–87.

Lu, C., Ren, D., Wang, X., Ha, T., Liu, L., Lee, E.J., Hu, J., Kalbfleisch, J., Gao, X., Kao, R., Williams, D., Li, C., 2014. Toll-like receptor 3 plays a role in myocardial infarction and ischemia/reperfusion injury. Biochim. Biophys. Acta 1842, 22–31.

Mauad, T., Hajjar, L.A., Callegari, G.D., da Silva, L.F., Schout, D., Galas, F.R., Alves, V.A., Malheiros, D.M., Auler Jr., J.O., Ferreira, A.F., Borsato, M.R., Bezerra, S.M., Gutierrez, P.S., Caldini, E.T., Pasqualucci, C.A., Dolhnikoff, M., Saldiva, P.H., 2010. Lung pathology in fatal novel human influenza A (H1N1) infection. Am. J. Respir. Crit. Care Med. 181, 72–79.